ACS APPLIED MATERIALS & INTERFACES

Research Article

www.acsami.org

New Strategy for Controlled Release of Drugs. Potential Pinpoint Targeting with Multiresponsive Tetraaniline Diblock Polymer Vesicles: Site-Directed Burst Release with Voltage

Yupeng Wu,[†] Siwei Liu,*[,†] Yangchun Tao,[†] Chunping Ma,[†] Yi Zhang,[†] Jiarui Xu,*[,†] and Yen Wei*[,‡]

[†]PCFM Lab, School of Chemistry and Chemical Engineering, Sun Yat-sen University, Guangzhou 51025, China

[‡]Department of Chemistry, Tsinghua University, Beijing 100084, China

Supporting Information

ABSTRACT: A series of amphiphlic diblock polymers, tetraaniline block with different length of poly(*N*-isopropylacrylamide) (TA-*b*-PNIPAM), have been successfully synthesized. In a suitable solution, the as-synthesized diblock polymers can form stable large compound vesicles (LCVs) with multiple bimolecular-layer structure through self-assembly. These factors, such as the block length, different organic solvent, solvent ratio, pH value, temperature, and voltage, which affect the morphology and properties of the assembled aggregates, are systematically investigated. When the degree of polymerization of PNIPAM block is close to 10, the as-synthesized diblock polymer may form stable LCVs with the uniform size as well as few defects in the mixed solvent of dimethylformamide/water (v/v = 3:7). The assembled LCVs possess the properties of triple-responsive capacity on temperature, pH, and voltage. Variation in any of these factors can cause some changes in the morphology of LCVs. The drug release properties for doxorubicin (DOX) loaded by LCVs affected by temperature, voltage, and different pH values have been investigated. It is interesting that the structure of LCVs can be destructed completely by applying a voltage at 0.6 V. With such an advantage, the drugs loaded by the LCVs could burst release into designated place by using appropriate circuit design or instrument, thus achieving maximum efficacy of the loaded drugs or other bioactive molecules without any unnecessary chemical substances added. This approach allows us to concentrate more on material design aspects only, without regard to the complex targeting issue which is the biggest obstacle of such materials in practical applications.

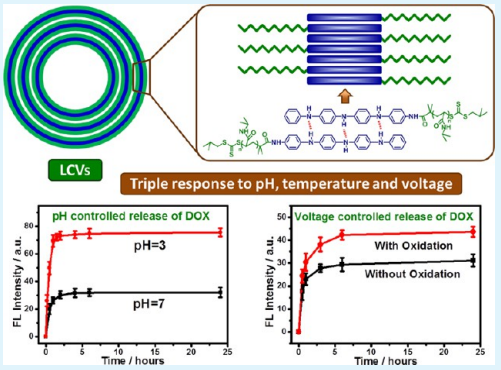

KEYWORDS: *tetraaniline diblock polymer, self-assembly, large compound vesicle, multiresponse, pinpoint targeting, drug release*

INTRODUCTION

Responsive polymer in the role of external stimuli can spontaneously adjust its own nature to adapt to the new surroundings,[1] such as regulating its amphiphilic nature,[2] controlling ion transport channel,[3] changing the chemical signals into optical, electrical, thermal or mechanical signals,[4] etc. The stimuli-responsive polymers, for this reason, have a broad range of applications in various aspects, such as drug release, medical diagnostics, tissue engineering, micromachine, biosensor, intelligent electrochemical system, smart coatings, etc.[5−14]

The responsive characteristics of the polymers in accordance with stimulation method can be divided into physical and chemical stimulation.[15] For example, the stimulation methods, such as by adjusting pH value, redox potential, ionic strength, and solvent polarity, belong to chemical stimulations, whereas changing the parameters, such as voltage, light, magnetism, and temperature, is generally attributed to physical methods. As a matter of fact, various properties of the materials, such as morphology, mechanical property, conductivity, light transmittance, and amphiphilic property, can be changed by the outside stimuli. As temperature, light, and pH value are often related to human life directly, a lot of the present research mainly focuses on temperature, light, and pH-responsive polymers.[16,17] In practical application, physical stimulation is generally superior to chemical methods, because it does not require any additional chemical substance to be added, which can prevent the subject investigated from destruction or turbulence.

Self-assembly is an important method in the preparation of supramolecules, as well as an effective means to synthesize new materials.[18−21] Nowadays, self-assembly as a technique to prepare stimuli-responsive polymeric aggregates by using amphiphilic block polymer as the basic element is becoming a hot research topic. In a suitable solution, the amphiphilic block polymer can form ordered self-assembled aggregates driven by the interaction between solvent molecules and the hydrophilic/hydrophobic blocks. Through appropriate molec-

Received: September 4, 2013
Accepted: January 22, 2014
Published: January 22, 2014

 © 2014 American Chemical Society dx.doi.org/10.1021/am404696u | ACS Appl. Mater. Interfaces 2014, 6, 1470−1480

ular design and optimal preparation conditions, the structure, functionality, and morphology of the self-assembled aggregates can be effectively controlled. Therefore, this technique has a wide range of potential applications in nano- and microscale reactors,[22−25] enzyme or catalyst nanocontainers,[26] template preparation for functional nanomaterials,[27] smart drug carriers,[28,29] and so forth.

The nature of temperature-responsive polymeric aggregates varies with the temperature changes.[30] Among temperature-responsive polymers, poly(*N*-isopropylacrylamide) (PNIPAM) is the most widely studied.[31−33] So far, researchers have developed a series of temperature-responsive aggregates with various polymers containing PNIPAM segment(s). O'Reilly's group reported a quaternary amine end functionalized diblock copolymer containing PNIPAM.[34] At room temperature, it could assemble into spherical micelles. However, it underwent a thermally induced morphology transition from micelles to vesicles above its lower critical solution temperature (LCST). Liu et al prepared the core cross-linked micelles possessing thermoresponsive cores.[35] The micelles were in a swollen state at room temperature. However, due to the collapse of PNIPAM block, the micelle size decreased above 40 °C. The micelles were used to detect mercury ions and they found that the detection sensitivity improved as the temperature increased. Liu and co-workers[36] reported the polymeric complex micelles prepared by self-assembly of poly(ε-caprolactone)-*block*-poly-(aspartic acid) (PCL-*b*-PAsp) and PCL-*b*-PNIPAM in water at room temperature, with PCL as the core and PAsp/PNIPAM as the mixed shell. As the temperature increased, PNIPAM collapsed and enclosed the PCL core, while PAsp penetrated through the PNIPAM shell, leading to the formation of negatively charged PAsp channels on the micelle surface. This system favored acquiring relatively steady plasma drug concentration, especially for ionic drugs. There are many similar reports by far.[37−41] In short, LCST is the key parameter for the kind of temperature sensitive materials (e.g., PNIPAM), and can be adjusted by introduction of other blocks. For PNIPAM, the LCST may reduce or even disappear by introducing hydrophobic blocks; conversely, the LCST will increase with the introduction of hydrophilic blocks. Therefore, by changing the LCST, one could design polymers with different transition temperatures to meet various application requirements.

The pH responsiveness of polymer aggregates refers to their physical and chemical properties varying with the changes of pH value. Usually, the typical pH-sensitive polymers containing ionizable components, with the abilities to give or accept protons, affect their solubility and the interaction between molecular chains, and ultimately control the aggregates morphology.[42] Borchert and co-workers reported a typical pH-responsive diblock copolymer, poly(2-vinylpyridine)-*block*-poly(ethylene oxide) (P2VP-*b*-PEO).[43] In water, it could form stable vesicles. Increasing acidity of the solution would cause the vesicle membrane rupture gradually, and the entire vesicle dissociation eventually. So, the substance encapsulated in the vesicles would be released. Kim's group[44] synthesized the pH-responsive polymeric micelles containing cancer targeted drugs. As the block polymer synthesized contained β-amino acids, when the pH value decreased, the micelles would gradually swell up and dissociate finally, resulting in the loaded drugs release. Zhong's group synthesized the pH-sensitive degradable chimaeric polymersomes based on asymmetric poly(ethylene glycol)-*b*-poly (2,4,6-trimethoxybenzylidene-1,1,1-tris-(hydroxymethyl) ethane methacrylate)-*b*-poly(acrylic acid) (PEG-PTTMA-PAA) triblock copolymers.[45] These chimaeric polymersomes could actively load doxorubicin (DOX) resulting in remarkably high drug loading contents and loading efficiencies. The in vitro release studies showed that DOX were released from chimaeric polymersomes in a controlled and pH-dependent manner.

By far, there are many reports on the investigation of pH, light, and temperature multiresponsive polymeric aggregates. But few articles focus on voltage stimulation on the vesicles concerning about the morphology changes and their applications. In general, the reported morphological changes of the polymeric aggregates require the addition of chemical substances. Compared to other stimulation methods, voltage stimulation has many advantages, such as easy remote and pinpoint control, few side effects, multiparameter regulation (voltage, current, time, pulsed voltage/current, etc.), and, the most important one, without any chemical substance addition. Kim et al. reported an amphiphile, tetraaniline block with poly(ethylene glycol).[46] In the aqueous solution, the morphology of the self-assembled aggregates could turn from vesicles to pucklike micelles while oxidized at 0.2 V. Interestingly, the pucklike micelles could regenerate vesicles after the solution reduced at −0.5 V. Nowadays, the targeting drug delivery characteristics make the delivery system design very complicated. It is difficult in practice to meet the requirements simultaneously in both aspects: targeting and delivery efficiency. However, to fabricate implantable and flexible microelectrodes is relatively easy.[47−49] So, the drug delivery system built by electroactive substance may not consider the targeting issue, just using tiny implantable electrodes to control drug release in vivo.

In this Article, by combining PNIPAM (temperature responsive block) and tetraaniline (TA, pH and voltage responsive block) into a single polymer, a series of amphiphilic diblock polymers has been synthesized, and their self-assembly properties were investigated. It was expected that, for the hydrophobic tetraaniline block, due to the amine−imine hydrogen bonding that only occurs in the emeraldine base (EB) state, the chain packs more compactly in the EB state than in the leucoemeraldine base (LEB) state.[46,50] Therefore, on one hand, the changes of pH values can weaken or enhance the hydrogen bond, thereby affecting the accumulation of the tetraaniline chain; and on the other, due to the excellent electroactive of aniline tetramer, the oxidation state can be controlled effectively by voltage, which in turn would affect the chain accumulation. As for the hydrophilic PNIPAM block, it is well-known as a temperature-responsive material. Driven by their own nature, the aggregates assembled by the as-synthesized polymer should have triple response capacity to temperature, pH value, and voltage. In a suitable mixed solvent, the as-synthesized diblock polymer could self-assemble into stable large compound vesicles (LCVs) with multiple bimolecular-layer structure. In this work, we have systematically studied the factors, such as the block length, different organic solvent, solvent ratio, pH value, temperature, and voltage, which would affect the morphology and properties of the assembled aggregates. Also, the loaded drugs, DOX, release properties, as well as the structural changes of LCVs in electric field were investigated.

EXPERIMENTAL SECTION

Materials. *N*-Phenyl-*p*-phenylenediamine (98%), phenylhydrazine (97%), 2-methyl-1-propanethiol (98%), methyltrioctylammonium chloride (MTOA, 99%), *N*-(3-dimethylaminopropyl)-*N*′-ethylcarbodiimide hydrochloride (EDC·HCl, 99%), and 4-dimethylaminopyridine (DMAP, 99%) were purchased from Aldrich and used as received. *N*-Isopropylacrylamide (NIPAM, 99%, Aldrich) was recrystallized twice from toluene/hexane (v/v = 1:10) at 50 °C and dried. 2,2-Azobisisobutyronitrile (AIBN) was purified by recrystallization twice from ethanol at 40 °C and dried in vacuum. Tetrahydrofuran (THF) and 1,4-dioxane were distilled over sodium prior to use, respectively. All solvents, such as acetone, carbon disulfide, dichloromethane, *n*-hexane, chloroform, dimethylformamide (DMF), dimethyl sulfoxide (DMSO), and other reagents (such as ferric chloride hexahydrate) were purchased from Guangzhou Chemical Reagent Co Ltd. and used as received.

Measurements. ^{1}H NMR spectra were performed on a Varian Unity Inova 300 spectrometer. Gel permeation chromatography (GPC) characterization was performed on a Waters Breeze at ambient temperature with THF as eluent against polystyrene standards. Fourier transform infrared (FTIR) spectra were recorded by using a Bruker EQUINOX 55 spectrometer via KBr tablet method. Thermogravimetric analyses (TGA) were performed with a thermal analyzer (TA Q50) under N_2 atmosphere with a heating rate of 10 °C/min. Scanning electron microscopy (SEM) images were obtained on a HITACHI S4800 microscope operated at 15 kV. Dynamic light scattering (DLS) measurements were conducted at 20−40 °C on a Brookhaven BI-200SM apparatus with a BI-9000AT digital correlator and a He−Ne laser at 532 nm. The samples were placed in an index-matching decal in a bath with temperature control within ±0.2 °C. The data were analyzed by CONTIN algorithm. The hydrodynamic diameter (D_h) and size polydispersity of the particles were obtained by cumulant analysis of the experimental correlation function. Conventional transmission electron microscopy (conventional-TEM) observations were performed on a transmission electron microscope (Philips TECNAI) with an accelerating voltage of 120 kV. To observe the original morphological sizes and geometries in aqueous solution, a drop of the prepared aggregate solution was deposited onto a carbon-coated copper grid. After a few minutes, the excess solution was blotted away with filter paper. Atomic force microscopy (AFM) of the aggregates was performed on a SPA300HV Probe station (Japan) in tapping mode. The samples were prepared by drying the aggregate solution on freshly cleaved mica at 25 °C. Cyclic voltammetry (CV) measurement was carried out on a Shanghai Chenhua electrochemical workstation CHI660C in a three-electrode cell with a Pt disk as counter electrode, an Ag/AgCl as reference electrode, and a glassy carbon as working electrode. UV−visible (UV−vis) absorption spectra were determined on a Hitachi U-3900 spectrophotometer. Fluorescence spectra were measured on a Shimadzu RF-5301PC spectrometer with a slit width of 3 nm for excitation and 5 nm for emission.

Synthesis of Tetraaniline (TA) in Leucoemeraldine Base (LEB). Tetraaniline was synthesized according to the pertinent literature.[51,52] Ferric chloride hexahydrate (27.03 g, 0.1 mol) was dissolved in hydrochloric acid (100 mL, 0.1 mol/L) at room temperature. *N*-Phenyl-*p*-phenylenediamine (18.40 g, 0.1 mol) was added to a 2.0 L flask equipped with 500 mL of 0.1 mol/L hydrochloric acid, stirring for 0.5 h. Then, the ferric chloride solution was added to the flask quickly in one portion while stirring constantly. The reaction mixture was filtered after 2 h and washed three times by 0.1 mol/L hydrochloric acid (300 mL) to remove ferric chloride. The filtrate was scattered in 500 mL ammonia (0.1 mol/L) for 3 h and then filtrated, washed with water 3 times, dried in vacuum oven for 48 h at 50 °C. The crude product was dissolved in ethanol and reduced to LEB with anhydrous phenylhydrazine. Then the final product was crystallized from ethanol to give off-white powder with the yield of 82% (13.10 g). ^{1}H NMR (300 MHz, DMSO-d_6, δ): 7.69 (s, 1H), 7.44 (s, 1H), 7.15 (t, 3H), 6.96−6.65 (m, 12H), 6.65 (t, 1H), 6.52 (d, 2H), 4.49 (s, 2H). FT-IR (KBr, cm^{-1}): 1598, 1529, 1513, 1307, 1155, 818, 748, 694. MS (EI) = 366.

Synthesis of the Chain Transfer Agent: *S*-1-Isobutyl-*S*′-(α,α′-dimethyl-α″-acetic acid)trithiocarbonate (IDAT).[53] Under argon atmosphere, the aqueous solution of sodium hydroxide (50 wt %, 4.0 mL) was added to the mixture of 2-methyl-1-propanethiol (4.8 mL), acetone (28 mL), and methyltrioctylammonium chloride (0.8 mL) at 5 °C. After the dropwise addition, stirring was continued for another 20 min. The carbon disulfide (2.8 mL in 8 mL acetone) was added to the mixture dropwise in 5 min. After 30 min, chloroform (5.6 mL) was added to the reaction mixture in one portion and following the aqueous solution of sodium hydroxide (50 wt %, 13 mL). Then the mixture was stirred at room temperature overnight. Water (65 mL) and concentrated hydrochloric acid (33 mL) were slowly added to adjust the mixture pH value to 1−2. The acetone in the mixture was removed by bubbling argon. Subsequently, the mixture was filtrated and the filtration was washed with water five times to remove salts. The final product, pale yellow crystal, was recrystallized from a mixture of acetone and *n*-hexane (v/v = 1:10) at the yield of 58% (6.50 g). ^{1}H NMR (300 MHz, $CDCl_3$, δ): 1.02 (d, 6H), 1.73 (s, 6H), 1.98 (s, 1H), 3.2 (d, 2H). FT-IR (KBr, cm^{-1}): 2957, 1701, 1065, 809.

Synthesis of Poly(*N*-isopropylacrylamide) (PNIPAM) Homopolymer. The as-synthesized chain transfer agent IDAT (0.51 g, 2 mmol), AIBN (catalytic amount) and NIPAM (2.26 g, 20 mmol) were dissolved in 1, 4-dioxane (10 mL) at room temperature, bubbling with argon for 15 min. The reactor was then placed in an oil bath at 70 °C and kept stirring. After 24 h, the reaction mixture was cooled down to room temperature and precipitated from *n*-hexane. The precipitate was dissolved in a small amount of THF and precipitated in *n*-hexane twice, and dried. The final product, pale yellow powdery solid, was obtained at the yield of 90% (2.47 g). ^{1}H NMR (300 MHz, $CDCl_3$, δ): 1.02 (*d*, $CH_2CH(CH_3)_2$), 1.16 (*s*, $NHCH(CH_3)_2$), 1.20−2.30 (*m*, $-C(CH_3)_2-$, $CH_2CH(CH_3)_2$ and the backbone protons of PNIPAM), 3.28 (*s*, SCH_2), 4.80 (*s*, NHC*H*), 7.30 (*bs*, CON*H*). FT-IR (KBr, cm^{-1}): 3434, 3327, 2972, 2933, 2874, 1647, 1545, 1461, 1172.

Synthesis of Tetraaniline-*block*-poly(*N*-isopropylacrylamide) (TA-*b*-PNIPAM). PNIPAM homopolymer (1.380 g, 1.0 mmol), EDC·HCl (0.287 g, 1.5 mmol) and catalytic amount of DMAP were dissolved into the mixture of dichloromethane/THF (20 mL, v/v = 3:2), while bubbling with argon for 15 min. Tetraaniline (0.549 g, 1.2 mmol) was added and the mixture was magnetic stirred for 24 h. Anhydrous phenylhydrazine (0.5 mL) and THF (5 mL) were added and the mixture was refluxed at 60 °C for 2 h. Then, the mixture was poured into *n*-hexane (200 mL). The precipitate was dissolved in 5 mL THF (the undissolved substances were filtered and discarded) and precipitated from 200 mL ether, and such the process was repeated at least five times. The final product as gray powder was obtained at the yield of 47% (0.82 g) and named as TA-PNI10. ^{1}H NMR (300 MHz, $CDCl_3$, δ): 1.02 (*d*, $CH_2CH(CH_3)_2$), 1.16 (*s*, $NHCH(CH_3)_2$), 1.20−2.30 (*m*, $-C(CH_3)_2-$, $CH_2CH(CH_3)_2$ and the backbone protons of in PNIPAM block), 3.28 (*s*, SCH_2), 4.80 (*s*, NHC*H*), 6.60−7.90 (*m*, −CON*H*− and the backbone protons of aromatic ring in tetraaniline block), 8.20 (*s*, Ar−N*H*−CO). FT-IR (KBr, cm^{-1}): 3416, 3301, 2972, 2933, 2874, 1647, 1545, 1509, 1463, 1305, 1172, 818, 748. By using the similar synthetic method, a series of the diblock polymers, TA-PNI15, TA-PNI20, TA-PNI30, and TA-PNI40, were synthesized. The only difference among these polymers is that, during the synthesis process of PNIPAM homopolymer, the ratio of NIPAM to chain transfer catalyst IDAT is different, that is, 10:1 for TA-PNI10, whereas 15:1, 20:1, 30:1 and 40:1 for TA-PNI15, TA-PNI20, TA-PNI30, and TA-PNI40, respectively.

Self-Assembly of the Diblock Polymer, TA-*b*-PNIPAM. The experimental procedure of self-assembly for TA-*b*-PNIPAM in solution is described as follows. For example, TA-PNI10 (4.0 mg) was dissolved in DMF (9 mL) completely aided by ultrasound. Then ultrapure water (21 mL) was added to the solution dropwise while rapidly stirring (500 rpm) for 10 min, and the mixture was kept stirring for another 5 min. The obtained emulsion was poured into a MWCO 3000 dialysis bag and then dialyzed for 3 days (the water was changed 2−3 times a day). Approximately 40 mL of emulsion (~0.1

Scheme 1. Synthetic Route for TA-*b*-PNIPAM Diblock Polymer

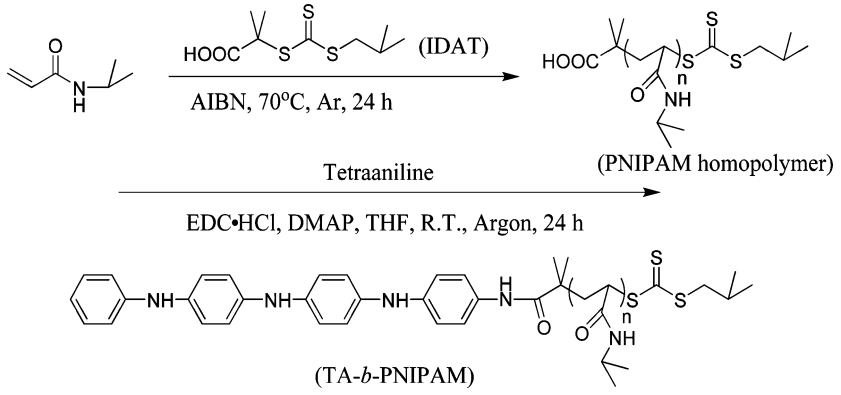

mg/mL) was obtained and stored in serum bottle for further use (similar self-assembly procedure for other diblock polymers we synthesized).

RESULTS AND DISCUSSION

Structural Characterization of TA-*b*-PNIPAM. In the presence of AIBN initiator, chain transfer agent, IDAT, was used for controlling the reversible addition−fragmentation chain transfer (RAFT) polymerization of NIPAM, to obtain a specific molecular weight with narrow weight distribution of PNIPAM. Subsequently, the as-synthesized PNIPAM homopolymer with carboxyl end group reacted with the amino group of tetraaniline by amidation to achieve the final diblock polymer, TA-*b*-PNIPAM (Scheme 1).

The ^{1}H NMR spectra of tetraaniline, PNIPAM and TA-*b*-PNIPAM are shown in Figure 1. For TA-*b*-PNIPAM, the new resonance absorption peak at 8.2 ppm indicates that the two blocks, tetraaniline and PNIPAM, are combined by an amide bond (−CONH−). In addition, the molecular weight calculated by ^{1}H NMR is consistent with the data obtained by GPC in the trend (see Supporting Information Table S1 and Figure S1). In the FT-IR spectra of tetraaniline (see Supporting Information Figure S2), a strong peak around 3392 cm^{-1} represents the stretching vibration absorption of N−H bond, and the peaks around 1598, 1529, and 1513 cm^{-1} are ascribed to the stretching vibration absorption of C−N bond. The peak at 818 cm^{-1} is due to the bending vibration absorption of C−H bond, and the peaks around 748 and 594 cm^{-1} can be attributed to the bending vibration absorption of C−H bond in the benzene ring. For PNIPAM, the peaks around 3434 and 3327 cm^{-1} represent the stretching vibration absorption of N−H bond. There are three peaks around 2972, 2933, and 2874 cm^{-1} which can be attributed to the vibration absorption peak for methyl, methylene and methine respectively. The peaks around 1647, 1545, 1461, and 1172 cm^{-1} can be ascribed to the absorption for C═O, N−H, CH_2, and C−N chemical bonds. For the diblock polymer TA-*b*-PNIPAM, the characteristic absorption peaks of the repeating unit NIPAM appear. Due to the introduction of the tetraaniline block, the stretching vibration absorption of N−H bond (amide) in PNIPAM block is shifted to lower wavenumber comparing to that of PNIPAM homopolymer. The characteristic C═C stretching vibration absorption peak of benzene ring appear at 1509 cm^{-1} as well as the peaks at 818 and 748 cm^{-1} are due to the C−H bending vibration absorption in bis-substituted and mono-substituted benzene ring respectively. All of the above data indicate that the target diblock polymer TA-*b*-PNIPAM has been successfully synthesized.

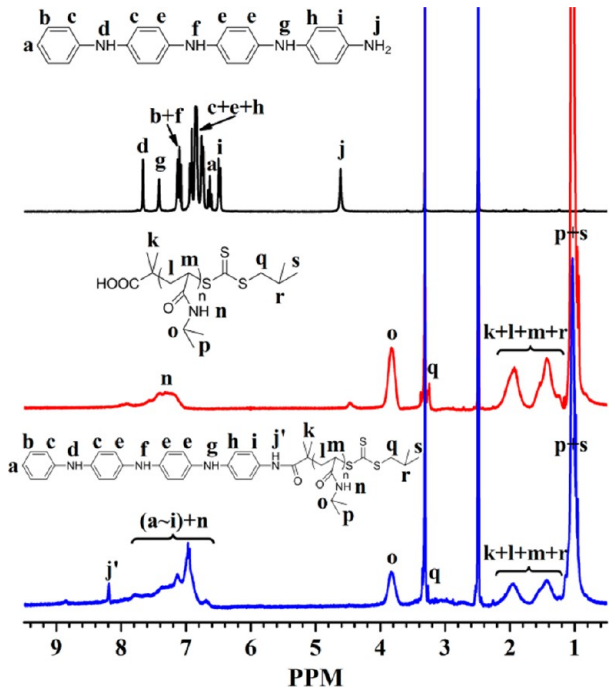

Figure 1. ^{1}H NMR spectra of tetraaniline, PNIPAM, and TA-*b*-PNIPAM (TA-PNI10) were recorded in DMSO-d_6. Each proton in these compounds has been assigned to each peak, and the assignments are marked on the diagram.

Tetraaniline has a good thermal stability, wherein at 310−405 °C the weight loss process for the thermal degradation of the main chain (see Supporting Information Figure S3). For the PNIPAM homopolymer, the thermal weight loss process can be divided into two stages. The first stage, from 200 to 290 °C, represents the degradation of the side chain, with approximately 19% of the weight loss. The second stage, from 290 to 400 °C, can be attributed to the main chain degradation process, the weight loss rate of 73% approximately. As for the diblock polymer, TA-*b*-PNIPAM, its thermogravimetric process can be divided into three stages, and the three fastest weight loss temperatures are 215, 252, and 394 °C, respectively. The first phase of the weight loss temperature is earlier than the PNIPAM homopolymer nearly 30 °C. The total weight loss in the first two stages is 42%, well above the PNIPAM homopolymer's the first phase of weight loss. Probably, this is due to the introduction of tetraaniline block

dx.doi.org/10.1021/am404696u | ACS Appl. Mater. Interfaces 2014, 6, 1470−1480

which increases the thermal conductivity of the diblock polymer; therefore, the heat is conducted to PNIPAM block more conveniently, accelerating the degradation.[54] The third stage, from 345 to 440 °C, can be ascribed to the degradation of the tetraaniline and the further degradation of PNIPAM block chain.

Self-Assembly of TA-*b*-PNIPAM Affected by Different Block Length of PNIPAM. The self-assembled aggregate morphologies of TA-PNI10 and TA-PNI15 have been investigated by AFM, SEM and TEM, as shown in Figure 2.

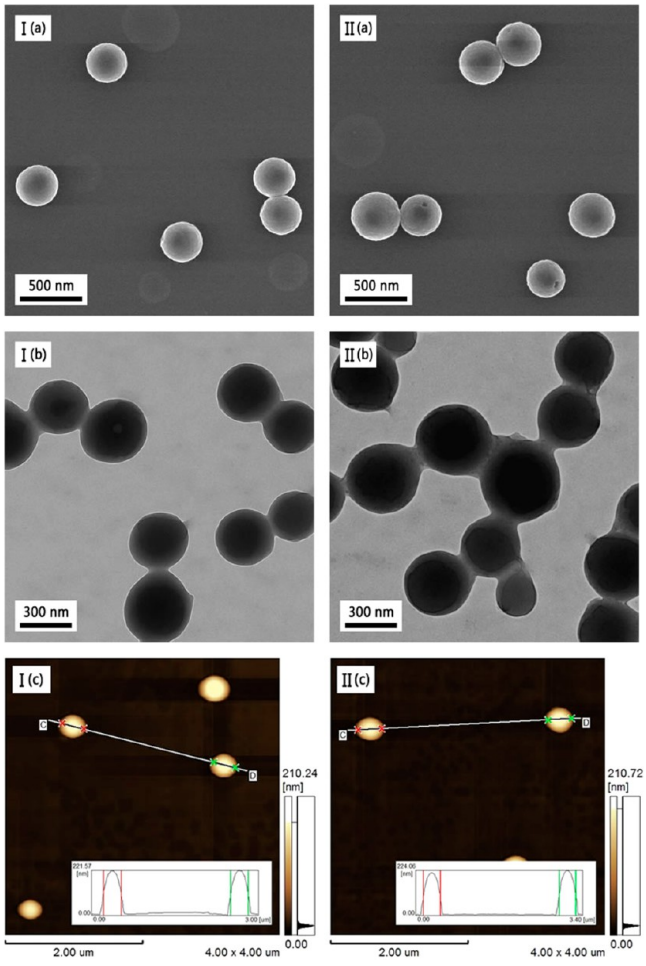

Figure 2. SEM (a), TEM (b), and AFM (c) images of the LCVs self-assembled by TA-PNI10 (I) and TA-PNI15 (II) in solution (v/v, DMF/water = 3:7), respectively.

In their optimal self-assembly condition, the diameter of the aggregates assembled by TA-PNI15 (360 nm) is larger than that of TA-PNI10 (320 nm). As the hydrophilic block PNIPAM is short in length, it is more likely that the polymer formed vesicles with a bimolecular-layer structure according to the theory of macromolecular self-assembly.[55] In our experiment, tapping-mode AFM observation shows that the aggregate is approximate 210 nm in height, indicating that the assembled aggregates might be stable LCVs having multiple bimolecular-layer structure,[56] as the single bimolecular-layer structure is easy to collapse while drying the samples. In other words, the assembled LCVs are not solid, but hollow; and the single wall thickness of the LCVs is about 105 nm. Compared to that of TA-PNI15, the aggregates assembled by TA-PNI10 are more uniform in size and have fewer defects. Nevertheless, both of them can self-assemble into stable LCVs in a suitable solvent. Probably this is due to both PNIPAM and tetraaniline blocks are substantially equal in length, resulting in very stable LCVs with bilayer structure. Based on these experimental evidence, here we propose a possible self-assembly mechanism illustrated as Scheme 2. In the self-assembly process, for tetraaniline block, due to its poor solvent (water) being added, the solubility in the mixed solvent is gradually deteriorated, whereupon tetraaniline blocks stack together side-by-side as the interlayer (hydrophobic layer), as well as with PNIPAM blocks as inner and outer layers (hydrophilic layer) through hydrogen bonding and $\pi-\pi$ stacking role, gradually forming a sandwich bimolecular-layer structure. Furthermore, during the self-assembly process, shear force generated by strong mixing makes the sandwich structure form stable vesicles or more stable LCVs through bending the sandwich bimolecular layers in several places, having a plurality of bimolecular-layer superposed on each other.[56] Additionally, we have further investigated how the block length of PNIPAM affects the aggregate morphology. There are many obvious holes in the LCVs assembled by TA-PNI20. It is probably due to the longer block length of PNIPAM (almost twice longer than TA-PNI10), which makes the bilayer structure of aggregates unstable, resulting more defects. As the block length of PNIPAM increases, no integrated LCVs can be assembled by TA-PNI30 and only small micelles exist as the aggregate morphology of TA-PNI40 (see Supporting Information Figure S4). In the following discussion of this Article, we will use the term TA-*b*-PNIPAN instead of TA-PNI10, unless otherwise specified, to investigate the properties and applications of the assembled LCVs.

Self-Assembly of TA-*b*-PNIPAM Affected by Different Organic Solvents. The general self-assembly process of the amphipathic diblock polymer is as follows in brief: polymer in organic solution is dispersed rapidly (e.g., by ultrasound or vigorous stirring) while adding water gradually; subsequently, the stable aggregates are assembled with a geometric appearance through noncovalent interactions (hydrogen bond, ionic bond, van der Waals force, hydrophobic interaction, etc.) by spontaneous organization or aggregation. During the process, both the polarity and viscosity of the organic solvents play essential roles in the formation of microstructure.[57−59] Therefore, the following four organic solvents with various polarity and/or viscosity are selected, ethanol, THF, DMF, and DMSO, in order to investigate how these factors affect the morphology of the assembled aggregates.

The morphology of the aggregates self-assembled in different organic solvent/water mixtures was studied by SEM separately (Figure 3). In the mixture of ethanol/water, there are two different forms of aggregates, one is LCVs with slight defects, and the other is smaller compound vesicles (or other kinds of aggregates) with diameter of 100−200 nm. Probably, due to the large polarity difference between ethanol and water, the chain of TA-*b*-PNIPAM undergoes strong driving force in the solution during mixing, resulting in the formation of compound vesicles with a smaller size.[57] Further, since the viscosity of ethanol is close to water, the mixed solvent has a stabilizing effect on the formed aggragates.[58,59] For THF/water mixture, some of the formed aggregates are bowl-shaped. Perhaps this is because of the weak polarity and low viscosity of THF, therefore resulting in many defective aggregates in the formation process. In the mixed solvent of DMF/water, due to the matched polarity and viscosity for each other, the

Scheme 2. Self-Assembling Mechanism of TA-*b*-PNIPAM

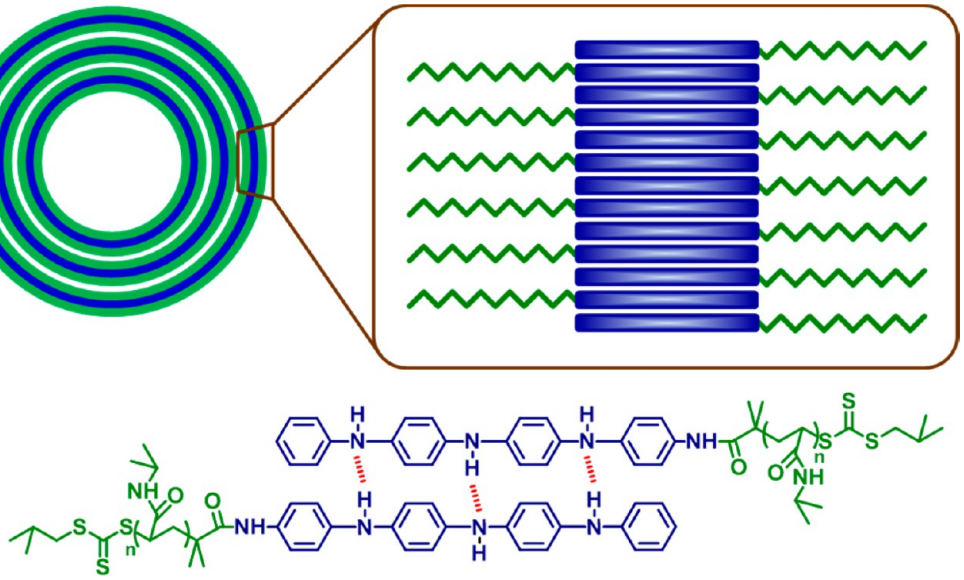

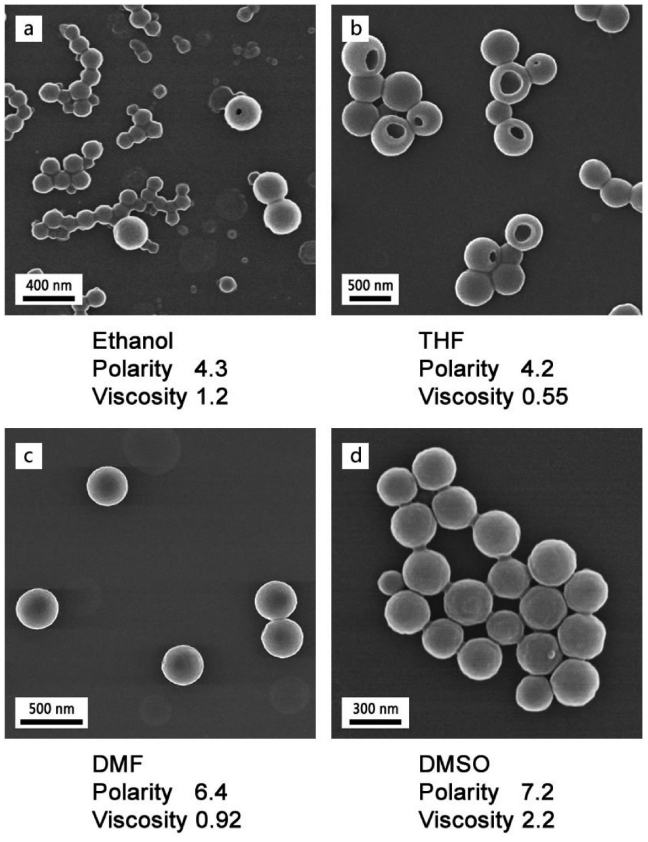

Figure 3. SEM images for the aggregates assembled by TA-*b*-PNIPAM in ethanol/H_2O (a), THF/H_2O (b), DMF/H_2O (c), and DMSO/H_2O (d). In all experiments, the volume ratio of organic solvent to water is 3:7. The polarity and viscosity of water are 10.2 and 1.0, respectively.

relatively perfect LCVs are obtained. As for the mixture of DMSO/water, although the polarity of the two solvents is similar, the viscosity varies greatly, which is not conducive to the accumulation of bimolecular layers. Therefore, the resulting aggregates have a certain degree of collapse.

Self-Assembly of TA-*b*-PNIPAM Affected by DMSO/Water Mixing Ratios. In mixed solvent, the driving force for amphiphilic polymer self-assembly is generated by the speed of water being added (poor solvent for the hydrophobic block) and the mixing ratio of organic solvent to water.[60,61] As described above, aggregates self-assembled in DMSO/water are stable due to high viscosity of DMSO. Here, we selected DMSO as the organic phase, with a fixed dripping speed of water at 2 mL/min, to investigate the effect of different DMSO/water mixing ratio (v/v) on the aggregate morphology (Figure 4). When the water content was 50%, the aggregates significantly stuck together, without any single isolated LCVs. However, when the proportion of water reached 60%, isolated

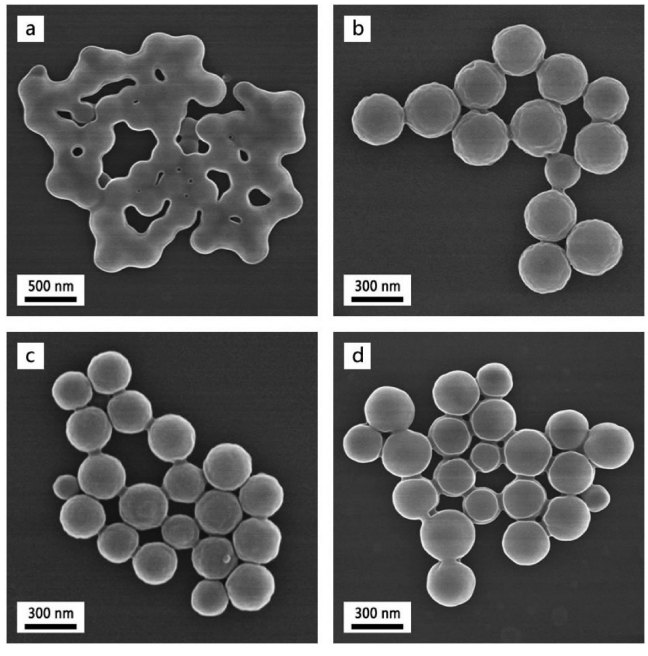

Figure 4. SEM images for the aggregates assembled by TA-*b*-PNIPAM in DMSO/water solvent which contained 50% H_2O (a), 60% H_2O (b), 70% H_2O (c), and 80% H_2O (d) (v/v).

dx.doi.org/10.1021/am404696u | *ACS Appl. Mater. Interfaces* 2014, 6, 1470−1480

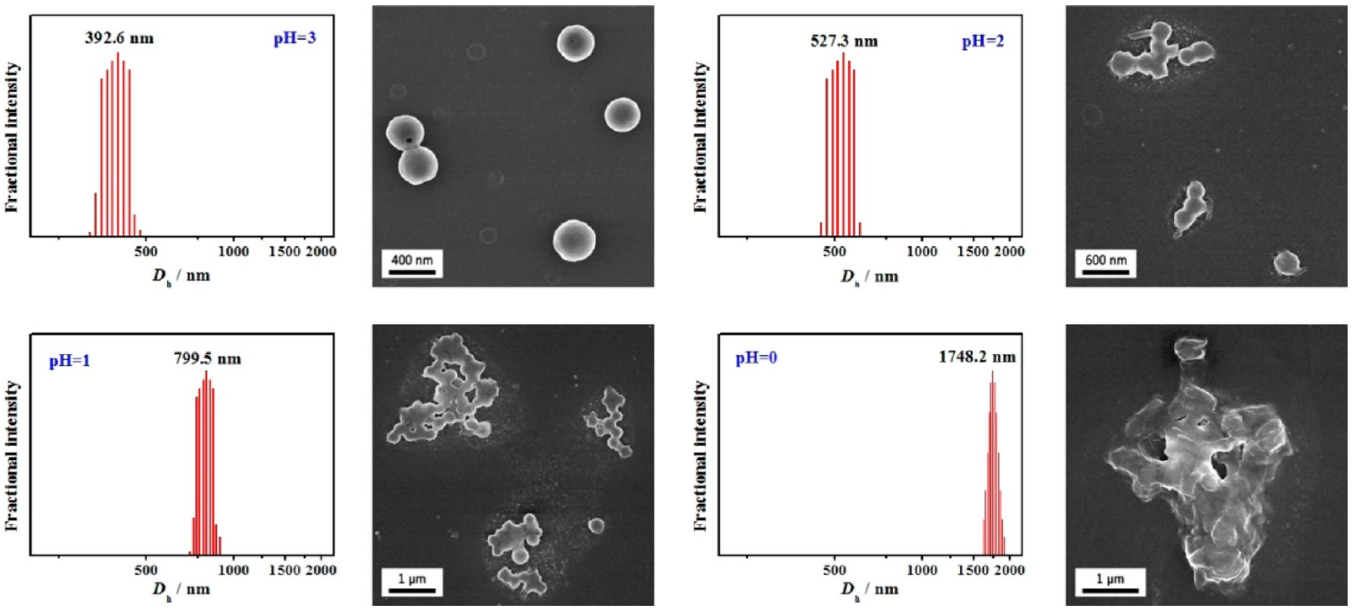

Figure 5. Morphology and size distribution of the LCVs self-assembled by TA-*b*-PNIPAM were determined by DLS and SEM at pH values of 3, 2, 1, and 0.

individual LCVs were obtained. Nevertheless, obvious collapse of LCVs could be found when the water proportion was 60%, 70% and 80%, respectively. Although the high viscosity makes the vesicles more stable, it will, in the meanwhile, decrease the superposition of the bilayer in LCVs. Therefore, the internal space between the bilayer increases and the LCVs are prone to collapse while increasing the proportion of water.

pH-Responsive Property of LCVs Assembled by TA-*b*-PNIPAM. Tetraaniline is similar to polyaniline in doping and dedoping characteristics.[62−64] By adjusting pH value of the self-assembled LCVs solution, we have scrutinized the changes in their sizes and morphologies. The diameter of the LCVs increases from 344.9 to 392.6 nm as the pH value decreases from 7 to 3. With the pH value decreases continuously, the diameter gradually increases, up to 1748.2 nm when the pH value reaches zero (see Supporting Information Figure S5). When the pH value is 3, the surface of LCVs collapses slightly and leads to some tiny holes, as compared with the LCVs at pH value of 7. This could be attributed to the small amount of hydrochloric acid added, which changes the doping state of tetraaniline blocks, increases the solubility (hydrophobic block) and then undermines the bilayer structure of the LCVs. The bilayer shell structure is further destroyed as the decrease of pH value. This process results in fusion of LCVs and therefore increases the particle diameter measured by DLS. When the pH value decreases to zero, the bilayer shell structure is almost completely destroyed, and thus, no LCV morphology could be found (Figure 5).

Through analyzing the data of both DLS and SEM images of the LCVs self-assembled by TA-*b*-PNIPAM, we can find that, as the pH value decreases from 7 to 3, the diameter increases about 46 nm, while the morphology of the LCVs remains unchanged (verified by their SEM images). When the pH value is held at 7, the diameter is in the range of 335−355 nm, and the diameter increases to the range of 380−395 nm when the pH value is adjusted to 3. It is very interesting that the diameter of the LCVs can be reversed through tuning pH value back to 7 by adding dilute ammonia solution. And such process can be repeated many times (Figure 6). In other word, the LCVs we prepared have a reversible response to pH value.

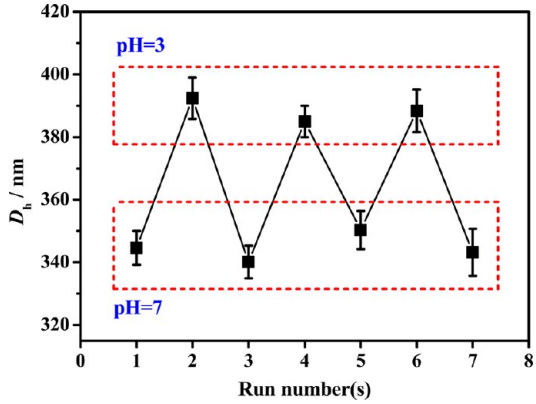

Figure 6. Hydrodynamic diameter (D_h) record for the LCVs assembled by TA-*b*-PNIPAM at pH of 7 and 3 in multiple consecutive pH runs.

As described above, by adjusting the pH value, the LCVs morphology self-assembled by TA-*b*-PNIPAM could be tuned. Taking advantage of this nature, we investigated the drug release properties for DOX. The experiment was carried out as follows: TA-*b*-PNIPAM (20 mg) and DOX (4 mg) were dissolved in DMF (5 mL). Then, water (15 mL) was added to the solution in 10 min dropwise. The obtained solution was divided equally into two and dialyzed against water. The water was changed every 2 h to remove the unloaded DOX. After 10 h, the two solutions were placed in 100 mL of water (pH = 7) and hydrochloric acid solution (pH = 3), respectively, to proceed with dialysis. The fluorescence spectra of the dialysate were monitored by fluorescence spectrophotometer and the peak intensity at 570 nm were plotted against time (Figure 7). The release rate of DOX is much higher in acid solution (pH = 3) than that in neutral solution. The total DOX release in acidic solution is also higher than the neutral system in 24 h. Probably

dx.doi.org/10.1021/am404696u | ACS Appl. Mater. Interfaces 2014, 6, 1470−1480

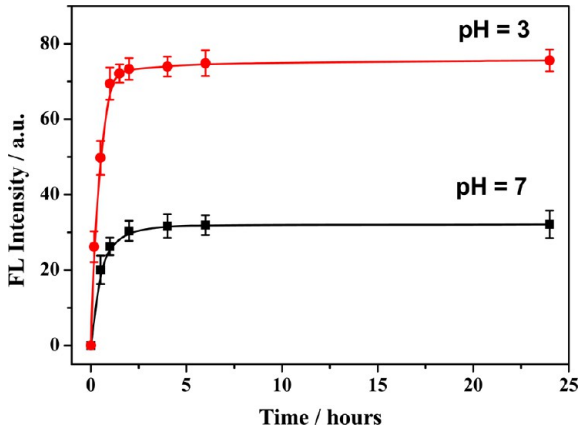

Figure 7. Peak intensity of fluorescence spectra at 570 nm versus time for the diaslysate of TA-*b*-PNIPAM/DOX at pH of 7 and 3.

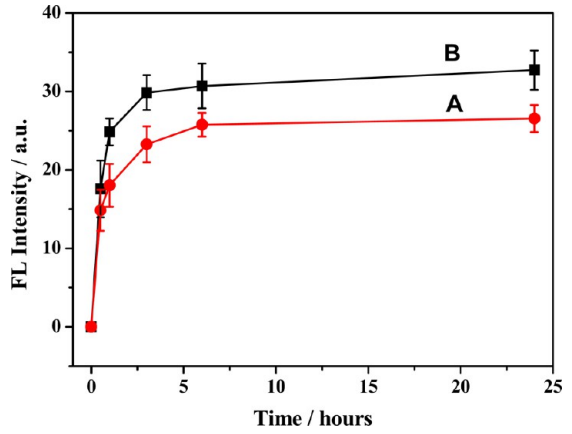

Figure 8. Peak intensity of fluorescence spectra at 570 nm versus time for the dialysate of TA-*b*-PNIPAM/DOX. (A) The LCVs solution was kept at a constant temperature of 36 °C by water bath; (B) the control experiment at 22 °C.

there are many cavities in the LCVs assembled by TA-*b*-PNIPAM to load DOX. When the bilayer structure of LCVs is not destroyed, it is not conducive to release the loaded DOX from the LCVs. However, when the solution acidity increases, the solubility of tetraaniline blocks is enhanced, which leads to a certain degree of damage of the bilayer structure, thereby accelerating the release of DOX, both in release rate and total release.

Temperature-Responsive Property of LCVs Assembled by TA-*b*-PNIPAM. It is well-known that PNIPAM is a temperature-sensitive polymer, soluble in cold water and insoluble above its LCST.[53,65] By using DLS, we measured the temperature responsive property of the LCVs self-assembled by TA-*b*-PNIPAN (see Supporting Information Figure S6). At 20 °C, the diameter is about 340 nm. As the temperature increases (from 20 to 26 °C), the diameter has no obvious changes. However, while the temperature rises from 26 to 30 °C, the diameter decreases rapidly to 305 nm. The size does not change significantly with further temperature increase. We thus believe that these changes are mainly due to a coil-to-globule phase transition of the PNIPAM block at its LCST.[65] Compared to PNIPAM homopolymer (31−33 °C), TA-*b*-PNIPAM has a lower LCST and broader transition. The decrease of LCST is probably due to the presence of a hydrophobic tetraaniline block, which lower the LCST of the PNIPAM. The expansion of the phase transition temperature may arise from the strong interchain interactions in the corona because of the crowding and repulsion between the neighboring PNIPAM blocks.[66,67]

As temperature increase can cause the LCVs shrink, we are curious about whether it may slow down the drug release when heating the solution above the LCST of TA-*b*-PNIPAM. Therefore, a parallel experiment of DOX release at a constant temperature of 22 and 36 °C was carried out respectively. As shown in Figure 8, the DOX release slows down when the temperature increases from 22 to 36 °C, indicating that the size shrinkage of LCVs in higher temperature may prevent DOX from releasing. As shown in Figure S6 in the Supporting Information, the diameter decreases dramatically only when the temperature increases from 26 to 30 °C. The diameter changes little while temperature is below 26 °C or above 30 °C. In other words, the DOX release property is similar when the temperature is greater than 30 °C or lower than 26 °C.

Voltage-Responsive Property of LCVs Assembled by TA-*b*-PNIPAM. Just as polyaniline, tetraaniline has good electrochemical activity and stability, having different oxidation states such as leucoemeraldine base (LEB), emeraldine base (EB) and pernigraniline base (PNB). And these different oxidation states can be transformed into each other by way of electrochemical redox, or adding oxidant/reductant and so forth.[68−70]

The LCVs solution self-assembled by TA-*b*-PNIPAM has two oxidation potentials in its CV curve (0.27 and 0.60 V), corresponding to its two oxidized state transitions (Figure 9). To the LCVs solution, a constant potential at 0.60 V (in order to destroy the vesicles structure) was powered for 4 h. We find that the oxidation potential at 0.60 V decreases to 0.58 V as well as the current increases from 2.2×10^{-6} to 2.9×10^{-6} A in the CV curves. We believe that these changes might be due to the transition from LEB state to higher oxidation state of the tetraaniline block under constant potential oxidation, resulting in higher conductivity (probably, after the oxidation, the accumulation of tetraaniline block becomes more compact because of the collapse of LCVs). Previous study showed that the TA block packs more compactly in EB state than in LEB state because of amine-imine hydrogen bonding occurs only in the EB form.[46] The different packing densities of TA blocks in different oxidation states resulted in different layer periodicities for the multilayered lamellar crystals. That is to say, the tilt angle between TA block and the other block of the block polymer is different in various oxidation states.[50] As we can see from the SEM image, the LCVs are destroyed and partially collapse to form disk aggregates (Figure 9) after being electrochemically oxidated for 4 h. That is to say, the assembled LCVs can be destroyed in electric field.

The drug release properties of LCVs affected by voltage have been investigated, as shown in Figure 10. When the neutral solution was electrochemically oxidated at 0.60 V, the release of DOX is faster than that in the control group without any electrochemical oxidation. Besides, total release of DOX in the oxidated group is around 39% higher than that in control group. However, total release of DOX during 24 h is lower than that obtained at a pH value of 3 without voltage stimuli. It could be speculated that some of the DOX is wrapped in the destruction of the LCVs. Nevertheless, these results indicate that the TA-*b*-PNIPAM/DOX system can release DOX more efficiently by electrochemical oxidation. Therefore, we could take advantage (by voltage response alone or plus pH and/or temperature response properties) of the LCVs to release loaded

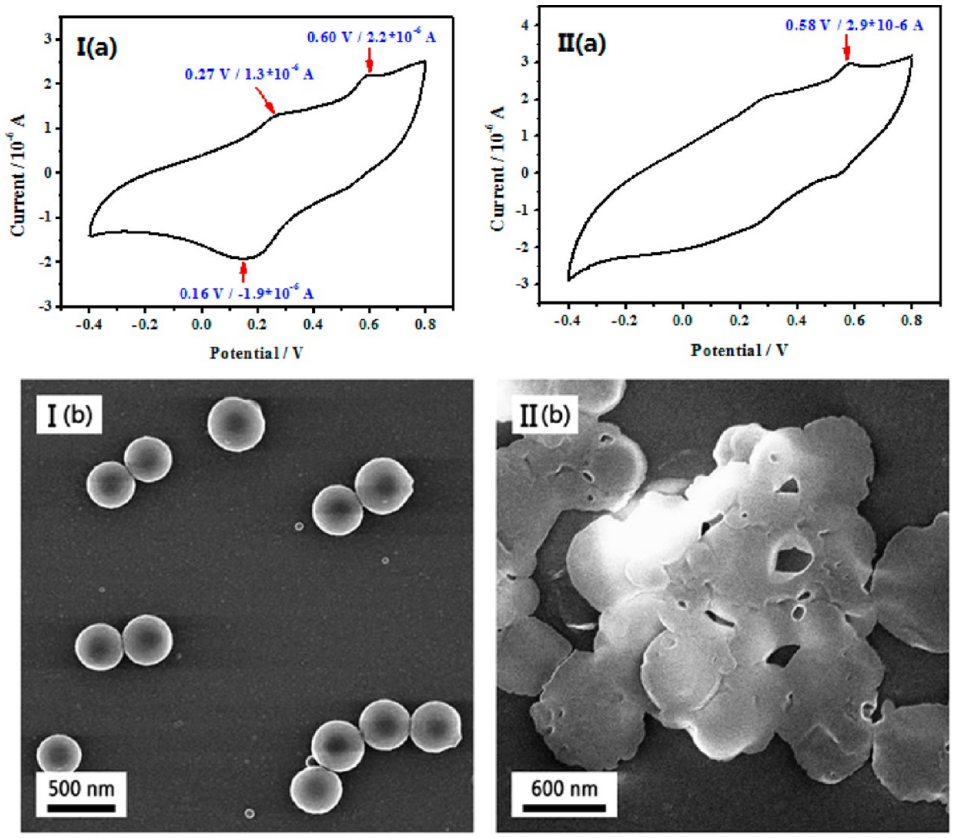

Figure 9. CV curves (a) and SEM images (b) for the LCVs assembled by TA-*b*-PNIPAM before (I) and after being electrochemically oxidized at 0.60 V for 4 h (II) with a concentration of 0.02 mg/mL in NaCl aqueous (0.05 mol/L) at the pH value of 7.

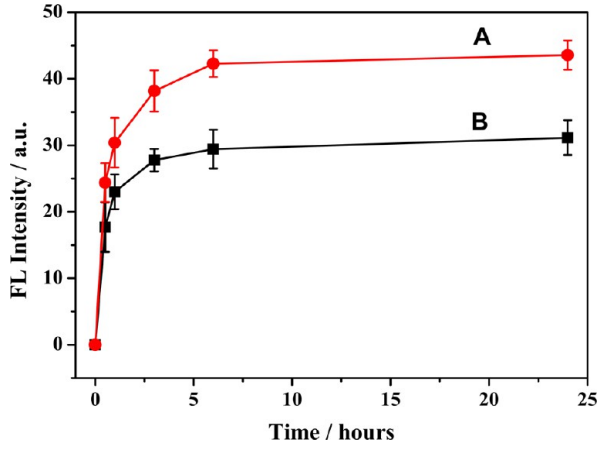

Figure 10. Peak intensity of fluorescence spectra at 570 nm versus time for the dialysate of TA-*b*-PNIPAM/DOX. NaCl aqueous solution (0.05 mol/L) was used as electrolyte as well as dialysate. (A) The LCVs solution was powered a constant potential at 0.60 V; (B) the control experiment.

drugs for site-directed burst release, in order to maximize drug efficacy through the implementation of fixed-point redox potential.

CONCLUSIONS

In summary, a new kind of diblock polymer, tetraaniline block with poly(*N*-isopropylacrylamide), possessing triple responsive properties on temperature, pH, and voltage, has been synthesized and fully investigated. In suitable mixed solvent (v/v, DMF/water = 3:7) and with appropriate length of PNIPAM block, the as-synthesized diblock polymer could form stable LCVs with multiple bimolecular-layer structure. The morphology of the self-assembled LCVs could be controlled by the block length of PNIPAM, the type of organic solvent, and the ratio of organic solvent to water. The triple response characteristics of the LCVs make the release of loaded drugs or bioactive molecules can be controlled in various ways. In particular, without using any chemical substances, the voltage-responsive property makes the stable LCVs a potential carrier for the burst release performance with drugs or other bioactive molecules. Specifically, the voltage control can be done remotely, accurate positioning, quantification, and so on. Accordingly, it would be practical to design a stable drug carrier, of which no drugs (or as little as possible) release in normal conditions; however, the loaded drugs or other bioactive molecules can be quantitatively released through voltage-stimuli according to actual requirements, thus maximizing utilization of these substances as well as reducing their side effects.

ASSOCIATED CONTENT

Supporting Information

FT-IR, TGA, and GPC data of the synthesized diblock polymers and their temperature responsive curves. This material is available free of charge via the Internet at http://pubs.acs.org.

AUTHOR INFORMATION

Corresponding Authors

*E-mail: liusiw@mail.sysu.edu.cn (S.L.).

*E-mail: xjr@mail.sysu.edu.cn (J.X.).
*E-mail: weiyen@tsinghua.edu.cn (Y.W.).

Notes

The authors declare no competing financial interest.

■ ACKNOWLEDGMENTS

This study was supported by the National Natural Science Foundation of China (No. 50903096), the Department of Science Technology of Guangdong Province (2008B090500196), and the Fundamental Research Funds for the Central Universities.

■ REFERENCES

(1) Stuart, M. A. C.; Huck, W. T. S.; Genzer, J.; Müller, M.; Ober, C.; Stamm, M.; Sukhorukov, G. B.; Szleifer, I.; Tsukruk, V. V.; Urban, M.; Winnik, F.; Zauscher, S.; Luzinov, I.; Minko, S. *Nat. Mater.* **2010**, *9*, 101−113.
(2) Sun, T.; Feng, L.; Gao, X.; Jiang, L. *Acc. Chem. Res.* **2005**, *38*, 644−652.
(3) Senaratne, W.; Andruzzi, L.; Ober, C. K. *Biomacromolecules* **2005**, *6*, 2427−2448.
(4) Liu, Z.; Calvert, P. *Adv. Mater.* **2000**, *12*, 288−291.
(5) Kelley, E. G.; Albert, J. N. L.; Sullivan, M. O.; Epps, T. H., III. *Chem. Soc. Rev.* **2013**, *42*, 7057−7071.
(6) Besnard, L.; Marchal, F.; Paredes, J. F.; Daillant, J.; Pantoustier, N.; Perrin, P.; Guenoun, P. *Adv. Mater.* **2013**, *25*, 2844−2848.
(7) Jäkle, F. *Chem. Rev.* **2010**, *110*, 3985−4022.
(8) Hoffman, A. S. *Adv. Drug Delivery Rev.* **2013**, *65*, 10−16.
(9) Nash, M. A.; Waitumbi, J. N.; Hoffman, A. S.; Yager, P.; Stayton, P. S. *ACS Nano* **2012**, *6*, 6776−6785.
(10) Tokarev, I.; Minko, S. *Soft Matter* **2012**, *8*, 5980−5987.
(11) Yoshida, R. *Biophysics* **2012**, *8*, 163−172.
(12) Gracia, R.; Mecerreyes, D. *Polym. Chem.* **2013**, *4*, 2206−2214.
(13) Li, G.; Zheng, Z.; Möhwald, H.; Shchukin, D. G. *ACS Nano* **2013**, *7*, 2470−2478.
(14) Kelly, J. C.; Pepin, M.; Huber, D. L.; Bunker, B. C.; Roberts, M. E. *Adv. Mater.* **2012**, *24*, 886−889.
(15) Zapotoczny, S. *Methods Mol. Biol.* **2012**, *811*, 51−78.
(16) Jochum, F. D.; Theato, P. *Chem. Soc. Rev.* **2013**, *42*, 7468−7483.
(17) Zhang, J.; Liu, H.; Yuan, Y.; Jiang, S.; Yao, Y.; Chen, Y. *ACS Macro Lett.* **2013**, *2*, 67−71.
(18) Habibi, Y.; Lucia, L. A.; Rojas, O. J. *Chem. Rev.* **2010**, *110*, 3479−3500.
(19) Yan, X.; Xu, D.; Chi, X.; Chen, J.; Dong, S.; Ding, X.; Yu, Y.; Huang, F. *Adv. Mater.* **2012**, *24*, 362−369.
(20) Liu, Y.; Yu, C.; Jin, H.; Jiang, B.; Zhu, X.; Zhou, Y.; Lu, Z.; Yan, D. *J. Am. Chem. Soc.* **2013**, *135*, 4765−4770.
(21) Kashem, M. M. A.; Patra, D.; Perlich, J.; Rothkirch, A.; Buffet, A.; Roth, S. V.; Rotello, V. M.; Buschbaum, P. M. *ACS Macro Lett.* **2012**, *1*, 396−399.
(22) Kazakov, S.; Kaholek, M.; Teraoka, I.; Levon, K. *Macromolecules* **2002**, *35*, 1911−1920.
(23) Nardin, C.; Widmer, J.; Winterhalter, M.; Meier, W. *Eur. Phys. J. E: Soft Matter Biol. Phys.* **2001**, *4*, 403−410.
(24) Wang, C.; Oskooei, A.; Sinton, D.; Moffitt, M. G. *Langmuir* **2010**, *26*, 716−723.
(25) Hatch, A. C.; Fisher, J. S.; Pentoney, S. L.; Yang, D. L.; Lee, A. P. *Lab Chip* **2011**, *11*, 2509−2517.
(26) Kim, K. T.; Meeuwissen, S. A.; Nolte, R. J. M.; van Hest, J. C. M. *Nanoscale* **2010**, *2*, 844−858.
(27) Shi, Z.; Zhou, Y.; Yan, D. *Macromol. Rapid Commun.* **2008**, *29*, 412−418.
(28) Thompson, C. J.; Ding, C.; Qu, X.; Yang, Z.; Uchegbu, I. F.; Tetley, L.; Cheng, W. *Colloid Polym. Sci.* **2008**, *286*, 1511−1526.
(29) Rösler, A.; Vandermeulen, G. W. M.; Klok, H. A. *Adv. Drug Delivery Rev.* **2012**, *64*, 270−279.
(30) Dimitrov, I.; Trzebicka, B.; Müller, A. H. E.; Dworak, A.; Tsvetanov, C. B. *Prog. Polym. Sci.* **2007**, *32*, 1275−1343.
(31) Luo, Y.; Yu, W.; Xu, F.; Zhang, L. *J. Polym. Sci., Part A: Polym. Chem.* **2012**, *50*, 2053−2067.
(32) Königer, A.; Plack, N.; Köhler, W.; Siebenbürger, M.; Ballauff, M. *Soft Matter* **2013**, *9*, 1418−1421.
(33) Nakayama, M.; Yamada, N.; Kumashiro, Y.; Kanazawa, H.; Yamato, M.; Okano, T. *Macromol. Biosci.* **2012**, *12*, 751−760.
(34) Moughton, A. O.; O'Reilly, R. K. *Chem. Commun.* **2010**, *46*, 1091−1093.
(35) Wan, X.; Liu, T.; Liu, S. *Langmuir* **2011**, *27*, 4082−4090.
(36) Liu, X.; Ma, R.; Shen, J.; Xu, Y.; An, Y.; Shi, L. *Biomacromolecules* **2012**, *13*, 1307−1314.
(37) Roy, D.; Nehilla, B. J.; Lai, J. J.; Stayton, P. S. *ACS Macro Lett.* **2013**, *2*, 132−136.
(38) Deka, S. R.; Quarta, A.; Corato, R. D.; Riedinger, A.; Cingolani, R.; Pellegrino, T. *Nanoscale* **2011**, *3*, 619−629.
(39) He, X.; Wu, X.; Gao, C.; Wang, K.; Lin, S.; Huang, W.; Xie, M.; Yan, D. *React. Funct. Polym.* **2011**, *71*, 544−552.
(40) Tang, Y.; Liu, L.; Wu, J.; Duan, J. *J. Colloid Interface Sci.* **2013**, *397*, 24−31.
(41) Qiao, J.; Qi, L.; Shen, Y.; Zhao, L.; Qi, C.; Shangguan, D.; Mao, L.; Chen, Y. *J. Mater. Chem.* **2012**, *22*, 11543−11549.
(42) Zhu, Z.; Armes, S. P.; Liu, S. *Macromolecules* **2005**, *38*, 9803−9812.
(43) Borchert, U.; Lipprandt, U.; Bilang, M.; Kimpfler, A.; Rank, A.; Süss, R. P.; Schubert, R.; Lindner, P.; Förster, S. *Langmuir* **2006**, *22*, 5843−5847.
(44) Wu, X. L.; Kim, J. H.; Koo, H.; Bae, S. M.; Shin, H.; Kim, M. S.; Lee, B. H.; Park, R. W.; Kim, I. S.; Choi, K.; Kwon, I. C.; Kim, K.; Lee, D. S. *Bioconjugate Chem.* **2010**, *21*, 208−213.
(45) Du, Y.; Chen, W.; Zheng, M.; Meng, F.; Zhong, Z. *Biomaterials* **2012**, *33*, 7291−7299.
(46) Kim, H.; Jeong, S. M.; Park, J. W. *J. Am. Chem. Soc.* **2011**, *133*, 5206−5209.
(47) Hoag, H. *Nature* **2003**, *423*, 796−798.
(48) Stieglitz, T. *Sens. Actuators, A* **2001**, *90*, 203−211.
(49) Stieglitz, T.; Meyer, J. U. *Med. Device Tech.* **1999**, *10*, 28−30.
(50) Kim, H.; Park, J. W. *J. Mater. Chem.* **2010**, *20*, 1186−1191.
(51) Zhang, W. J.; Feng, J.; MacDiarmid, A. G.; Epstein, A. J. *Synth. Met.* **1997**, *84*, 119−120.
(52) Wei, Y. *J. Chem. Educ.* **2001**, *78*, 551−553.
(53) Kujawa, P.; Segui, F.; Shaban, S.; Diab, C.; Okada, Y.; Tanaka, F.; Winnik, F. M. *Macromolecules* **2006**, *39*, 341−348.
(54) Gupta, N.; Kumar, D.; Tomar, S. K. *Int. J. Mater. Chem.* **2012**, *2*, 79−85.
(55) Bates, F. S.; Fredrickson, G. H. *Annu. Rev. Phys. Chem.* **1990**, *41*, 525−557.
(56) Yu, K.; Eisenberg, A. *Macromolecules* **1998**, *31*, 3509−3518.
(57) Yu, Y.; Zhang, L.; Eisenberg, A. *Macromolecules* **1998**, *31*, 1144−1154.
(58) Zang, L.; Che, Y.; Moore, J. S. *Acc. Chem. Res.* **2008**, *41*, 1596−1608.
(59) Podlogar, F.; Gašperlin, M.; Tomšič, M.; Jamnik, A.; Rogač, M. B. *Int. J. Pharm.* **2004**, *276*, 115−128.
(60) Yu, Y.; Zhang, L.; Eisenberg, A. *Langmuir* **2001**, *17*, 6705−6714.
(61) Burke, S. E.; Eisenberg, A. *Polymer* **2001**, *42*, 9111−9120.
(62) Shao, Z.; Yu, Z.; Hu, J.; Chandrasekaran, S.; Lindsay, D. M.; Wei, Z.; Faul, C. F. J. *J. Mater. Chem.* **2012**, *22*, 16230−16234.
(63) Ford, W. E.; Gao, D.; Scholz, F.; Nelles, G.; Wrochem, F. V. *ACS Nano* **2013**, *7*, 1943−1951.
(64) Basavaiah, K.; Rao, A.V. P. *E-J. Chem.* **2012**, *9*, 1175−1180.
(65) Zhang, G.; Wu, C. *Adv. Polym. Sci.* **2006**, *195*, 101−176.
(66) Zhang, W.; Zhou, X.; Li, H.; Fang, Y.; Zhang, G. *Macromolecules* **2005**, *38*, 909−914.
(67) Li, J.; He, W.; Sun, X. *J. Polym. Sci., Part A: Polym. Chem.* **2007**, *45*, 5156−5163.
(68) Chen, L.; Yu, Y.; Mao, H.; Lu, X.; Zhang, W.; Wei, Y. *Mater. Lett.* **2005**, *59*, 2446−2450.

(69) Wei, Z.; Faul, C. F. J. *Macromol. Rapid Commun.* **2008**, *29*, 280−292.
(70) Udeh, C. U.; Fey, N.; Faul, C. F. J. *J. Mater. Chem.* **2011**, *21*, 18137−18153.